Biogeosciences, 4, 505–519, 2007
www.biogeosciences.net/4/505/2007/

Biogeosciences

The fate of pelagic $CaCO_3$ production in a high CO_2 ocean: a model study

M. Gehlen[1], R. Gangstø[1], B. Schneider[1], L. Bopp[1], O. Aumont[2], and C. Ethe[1]

[1]LSCE/IPSL, Laboratoire des Sciences du Climat et de l'Environnement, CEA-CNRS-UVSQ, Orme des Merisiers, Bât. 712, CEA/Saclay, 91198 Gif-sur-Yvette Cedex, France
[2]LOCEAN/IPSL, Centre IRD de Bretagne, BP 70, 29280 Plouzané, France

Received: 6 February 2007 – Published in Biogeosciences Discuss.: 12 February 2007
Revised: 20 June 2007 – Accepted: 2 July 2007 – Published: 13 July 2007

Abstract. This model study addresses the change in pelagic calcium carbonate production ($CaCO_3$, as calcite in the model) and dissolution in response to rising atmospheric CO_2. The parameterization of $CaCO_3$ production includes a dependency on the saturation state of seawater with respect to calcite. It was derived from laboratory and mesocosm studies on particulate organic and inorganic carbon production in *Emiliania huxleyi* as a function of pCO_2. The model predicts values of $CaCO_3$ production and dissolution in line with recent estimates. The effect of rising pCO_2 on $CaCO_3$ production and dissolution was quantified by means of model simulations forced with atmospheric CO_2 increasing at a rate of 1% per year from 286 ppm to 1144 ppm over a 140 year time-period. The simulation predicts a decrease of $CaCO_3$ production by 27%. The combined change in production and dissolution of $CaCO_3$ yields an excess uptake of CO_2 from the atmosphere by the ocean of 5.9 GtC over the period of 140 years.

1 Introduction

About 50% of the CO_2 released by human activity since the beginning of the industrialization has accumulated in the atmosphere (Feely et al., 2004). The other half of the total release was taken up by the terrestrial biosphere (20%) and the ocean (30%). The world ocean is thus the largest sink for anthropogenic CO_2, with a total uptake of 118±19 Pg C between 1800 and 1994 (Sabine et al., 2004). In seawater CO_2 behaves like a weak acid. The associated chemical reactions drive a decrease in pH (increase in acidity) and in carbonate ion concentration ($CO_2+H_2O+CO_3^{2+} \leftrightarrow 2HCO_3^-$). This process known as acidification (e.g. Caldeira and Wickett, 2003; Feely et al., 2004; Orr et al., 2005) decreases the saturation state of seawater with respect to calcium carbonate ($CaCO_3$). The saturation state is defined as the ratio of the in situ ion concentration product $[Ca^{2+}]\times[CO_3^{2-}]$ over the stoichiometric solubility product Ksp (Mucci, 1983):

$$\Omega = \frac{\left[Ca^{2+}\right] \times \left[CO_3^{2-}\right]}{\mathrm{Ksp}} \quad (1)$$

In the modern ocean, abiotic $CaCO_3$ precipitation is only a minor contribution to total carbonate production. The majority of $CaCO_3$ is produced by organisms: e.g. coralline algae (high-Mg calcite), pteropods and corals (aragonite), bivalves (calcite, aragonite, mixed calcite and aragonite), coccolithophores (calcite), foraminifera (mostly calcite, but also aragonite). The solubility decreases from high-Mg calcite, and aragonite to calcite suggesting differing degrees of vulnerability of organisms to ocean acidification. While the exact reaction pathway of biocalcification awaits further elucidation for most calcifiers, it has been shown to strongly depend on the level of supersaturation. In general, calcification decreases with decreasing saturation state (refer to Kleypas et al. (2006) for a comprehensive synthesis of existing data). While calcification appears to be linearly related to the saturation state in corals, experimental results obtained for foraminifera and coccolithophores suggest the existence of a threshold value of saturation state below which the calcification will decrease drastically (e.g. Gattuso et al., 1998; Bijma et al, 1999; Kleypas et al., 1999; Riebesell et al., 2000; Zondervan et al., 2001; Zondervan et al., 2002). Unmitigated acidification of oceanic waters will ultimately threaten the existence of marine calcifiers and cause major changes in marine ecosystems.

In terms of feedback on rising atmospheric CO_2, three distinct yet interconnected groups of processes involving $CaCO_3$ can be identified:

Correspondence to: M. Gehlen
(marion.gehlen@cea.fr)

Published by Copernicus Publications on behalf of the European Geosciences Union.

1. Calcification: $CaCO_3$precipitation leads to a pCO_2 increase according to Eq. (2):

$$Ca^{2+} + 2HCO_3^- \leftrightarrow CaCO_3 + CO_2 + H_2O \quad (2)$$

A decrease in calcification would thus favor the uptake of atmospheric CO_2 by the ocean and acts as a negative feedback on rising atmospheric pCO_2. A potential decrease of surface ocean pCO_2 of 10 to 20 μatm was estimated for a complete shutdown of surface ocean calcification (Gruber et al., 2004). The ratio of CO_2 released per mole of $CaCO_3$ precipitated is a function of the buffer capacity of the seawater acid-base CO_2 system. Under present conditions, roughly 0.6 moles of CO_2 are released per mole of $CaCO_3$ precipitated (Frankignoulle et al., 1994). This ratio will increase as the overall buffer capacity of seawater decreases in response to anthropogenic CO_2 uptake (Zeebe and Wolf-Gladrow, 2001), thereby counteracting the effect of decreasing calcification.

2. Dissolution: The effect of dissolution follows directly from the stoichiometry of Eq. (2) (backward reaction). Enhanced dissolution of $CaCO_3$ in response to acidification increases ocean alkalinity thereby favoring CO_2 uptake, which can be considered as a negative feedback on atmospheric pCO_2.

3. $CaCO_3$ export and rain ratio effect: A decrease in calcification will alter the ratio of organic C to inorganic C (the rain ratio): an increase in rain ratio will promote the dissolution of $CaCO_3$ in marine sediments resulting in a higher alkalinity (Archer and Maier-Reimer, 1994), a negative feedback operating on timescales of 10 000 years. Alternatively, if the ratio of organic C to inorganic C is closely bound by the process of ballasting (Ittekott, 1993; Armstrong et al., 2002; Klaas and Archer, 2002), less $CaCO_3$ production would imply less ballasting of organic C (POC) fluxes and a shallower remineralization of POC which corresponds to a positive feedback on atmospheric CO_2.

The interplay between these processes makes it difficult to have an a priori knowledge of the amplitude and sign of the feedback associated with changes in the carbonate chemistry of seawater and calcification/dissolution/ballasting in response to ocean acidification. The present model study focuses on the response of calcification (1) and $CaCO_3$ dissolution (2) to rising pCO_2, but not on the rain ratio effect (3). The aim is, on one hand, to quantify the calcification/dissolution feedback on rising atmospheric CO_2, on the other, to assess the relative importance of the two individual processes.

2 Model description

2.1 The biogeochemical model PISCES: a brief general description

The biogeochemical model PISCES (Aumont et al., 2003; Aumont and Bopp, 2006; Gehlen et al., 2006) simulates the biogeochemical cycle of oxygen, carbon and of the main nutrients controlling marine phytoplankton growth: nitrate and ammonium, phosphate, silicate and iron. The nutrient concentration is linked through a constant Redfield ratio and phytoplankton growth is limited by the external availability of nutrients. The cycles of carbon and nitrogen are decoupled in the model to a certain degree by nitrogen fixation and denitrification. The model distinguishes two phytoplankton size-classes corresponding to nanophytoplankton and diatoms, and two zooplankton size classes which are microzooplankton and mesozooplankton. For all species, the C/N/P ratios are assumed constant. The prognostic variables of phytoplankton are total biomass, iron, chlorophyll and silicon contents. The internal ratios of Fe/C, Chl/C and Si/C of phytoplankton are predicted by the model. For zooplankton, the total biomass is the only prognostic variable. The bacterial pool is not modeled explicitly. The model distinguishes three non-living compartments for organic carbon: semi- labile dissolved organic carbon (DOC) with timescales of several weeks to several years, two size classes of particulate organic carbon (small particles = POCs and big particles = POCb). While the C/N/P composition of dissolved and particulate matter is tied to Redfield stochiometry, the iron, silicon and carbonate contents of the particles are diagnosed.

The two particulate detrital pools (POCs and POCb) are fueled by mortality, aggregation from nanophytoplankton and diatoms, fecal pellet production and grazing. Mineralization of particulate organic carbon together with excretion contributes to the semi-labile pool of dissolved organic carbon. Differential settling and turbulence promote particle aggregation. The parameterization of aggregation is based on Jackson (1990) and Kriest and Evans (1999, 2000). Small particles sink with a constant sinking speed of 3 m/d. Large particles, as well as $CaCO_3$ and SiO_2 sink with a sinking speed increasing with depth from 50 m/d at the base of the mixed layer to 200 m/d at 2000 m, respectively 425 m/d at 5000 m depth.

A detailed description of PISCES, including model equations and parameters is available as supplementary material in Aumont and Bopp (2006). We present hereafter a description of $CaCO_3$ production and dissolution. These parameterizations were adapted for the scope of the present study.

2.2 Biogeochemical cycle of carbonate in PISCES

PISCES simulates dissolved inorganic carbon and total alkalinity (carbonate alkalinity + borate + water). The carbon chemistry is computed following the OCMIP protocols (http://www.ipsl.jussieu.fr/OCMIP).

2.2.1 Carbonate production

Several phyla contribute to pelagic $CaCO_3$ production. Together with calcite producing coccolithophores and foraminifera, aragonite secreting pteropods make up for the

majority of planktonic $CaCO_3$ production (Kleypas et al., 2006). Quality data on the distribution and abundances of these taxa are scarce and large uncertainties are associated with estimates of their contribution to pelagic calcification. Foraminifera and coccolithophores are believed to be the main contributors (Schiebel, 2002), leaving between 4 to 13% of $CaCO_3$ production to be attributed to pteropods (Fabry, 1989; Fabry, 1990). The partition between coccolithophores and foraminifera is poorly constrained. According to Schiebel (2002), the latter may contribute up 23–56% of the $CaCO_3$ flux at 100 m (Schiebel et al., 2002). While experimental studies with representatives of all three groups of calcifiers gave evidence for a calcification response to changes in the carbonate system, the majority of data were collected for coccolithophores (Kleypas et al., 2006). Facing the scarcity of experimental data and in order to allow a first assessment of the calcification/dissolution feedback on rising atmospheric CO_2, we decided to attribute pelagic calcification to calcite secreting coccolithophores. Our approach is extended to aragonite producing pteropods in a follow-up study by Gangstø et al. (2007)[1].

Marine calcifiers are not implemented as a distinct plankton functional group in PISCES. In the model standard version, carbonate production is assigned to nanophytoplankton, the size class of coccolithophores, as a function of temperature and nutrient levels. Parameter values controlling $CaCO_3$ production were chosen such as to reproduce the general distribution patterns of coccolithophores (Moore et al., 2002; Aumont and Bopp, 2006). For the purpose of this study, the standard parameterization of $CaCO_3$ formation was updated to account for the saturation state of ambient waters with respect to calcite based on a synthesis of experimental studies.

The bloom-forming cosmopolitan species *Emiliania huxleyi* was used in a large number of studies addressing the effect of increasing atmospheric pCO_2 on the production of calcite and the particulate inorganic carbon (PIC) to particulate organic carbon (POC) ratio. Experimental studies encompass laboratory experiments with monospecific cultures of *E. huxleyi* (Riebesell et al., 2000; Sciandra et al., 2003; Zondervan et al., 2001, 2002) and results from a mesocosm experiment with a natural phytoplankton population dominated by this calcifying species (Delille et al., 2005). All studies document a decrease in calcification with increasing pCO_2. The response in terms of the PIC to POC ratio is more differentiated and depends on light and nutrient conditions. Under N-limited growth conditions, Sciandra et al. (2003) report constant PIC to POC ratios for *E. huxleyi* cultures grown under elevated pCO_2. The constant PIC to POC ratio results from the concomitant decrease in inorganic carbon and organic carbon production. In contrast, experiments with nutrient replete *E. huxleyi* cultures (Riebesell et al., 2000; Zondervan et al., 2001, 2002) yielded a decrease in PIC/POC with increasing pCO_2 resulting from the combined effect of a decrease in inorganic carbon production and an increase in organic carbon synthesis. The same response was found during a mesocosm experiment with a natural phytoplankton population dominated by blooming *E. huxleyi* (Delille et al., 2005).

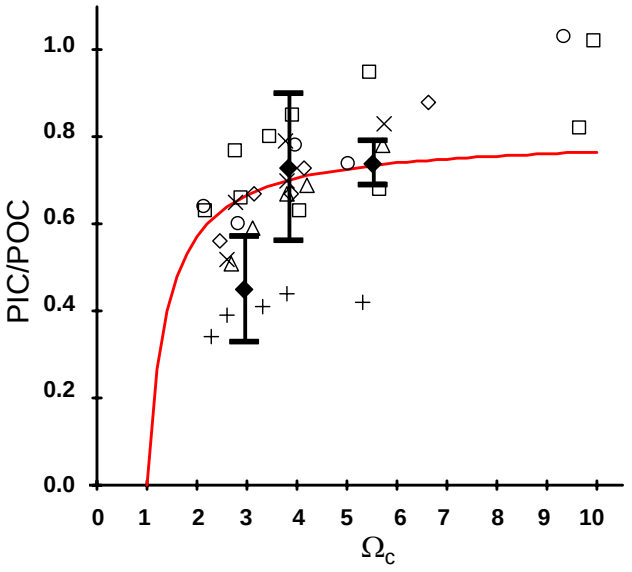

Fig. 1. The PIC/POC ratio as a function of the saturation state with respect to calcite, Ω_c. Open symbols, data by Zondervan et al. (2002). Closed diamonds, data by Delille et al. (2003). Solid line fit, obtained with Eq. (3) (r^2=0.9193).

We included only experimental data from N-replete experiments for the purpose of this model study (Delille et al., 2005; Riebesell et al., 2000; Zondervan et al., 2001, 2002). The saturation state of seawater with respect to calcite was computed from measured total alkalinity and pCO_2 using the CO2SYS Package (Lewis and Wallace, 1998) and carbonic acid dissociation constants by Mehrbach et al. (1973). Experimental PIC to POC ratios are plotted as a function of saturation of seawater with respect to calcite (Ω_c) in Fig. 1. All experiments document a qualitatively similar response to a decrease in saturation state Ω_c (Fig. 1). The scatter in the data reflects differences in experimental conditions (e.g. nutrient availability and light conditions). Due to the limited number of observations, all data were used to derive the parameterization describing the carbonate production as a function of Ω_c. Since the biocalcification underlies physiological controls, a Michaelis-Menten kinetic was selected for the dependency of the carbonate production – expressed as the ratio of PIC to POC – to the saturation state:

$$\frac{\mathrm{PIC}}{\mathrm{POC}} = \left(\frac{\mathrm{PIC}}{\mathrm{POC}}\right)_{\max} \times \frac{(\Omega_c - 1)}{K\,\max + (\Omega_c - 1)} \qquad (3)$$

[1]Gangstø, R., Gehlen, M., Bopp, L., Aumont, O., Schneider, B., and Joos, F.: Representing aragonite production and dissolution in a biogeochemical ocean model, Global Biogeochem. Cy., in review, 2007.

where: PIC/POC=ratio of inorganic to organic carbon; PIC/POC_{max}=0.8, maximum ratio observed under optimal growing conditions; Kmax=0.4, with analogy to the half saturation constant, value of (Ω_c-1) for which PIC/POC equals half of its maximal value.

The ratio PIC/POC max was chosen to equal 0.8. While in monospecific cultures values up to 1 might be encountered, the ratio PIC to POC in natural phytoplankton population does not exceed 0.8 even when coccolithophores are blooming (see Fig. 1 and corresponding references). The value of Kmax of 0.4 reflects the observation that for some marine calcifiers calcification decreases rapidly below a threshold value of Ω=4.0 (Gattuso et al., 1998).

Following the new parameterization, the model computes carbonate production as a function of environmental parameters (temperature, nutrient limitation and saturation state). We refer to this production as the *gross $CaCO_3$ production*. The pool of sinking carbonate particles is fueled by mortality and grazing on calcifying nanophytoplankton. Half of the grazed shells are routed to the sinking flux of $CaCO_3$, the other half is assumed to dissolve in the guts of grazers. The resulting carbonate flux corresponds to the *net $CaCO_3$ production*. This description was adopted in order to account for the observed, yet largely unexplained, loss of carbonate production in the upper ocean (Milliman et al., 1999).

2.2.2 Carbonate dissolution

The dissolution of $CaCO_3$ has been extensively studied over the past decades (e.g. Morse and Berner, 1972; Ingle et al., 1973; Berner and Morse, 1974; Berner, 1976; Morse, 1978; Honjo and Erez, 1978; Plummer et al., 1978; Keir, 1980; Walter and Morse, 1985; Chou et al., 1989; Arakaki and Mucci, 1995; Morse and Arvidson, 2002; Gehlen et al., 2005a, b). It is in general described by a higher order dependence of the dissolution reaction on the degree of undersaturation of seawater:

$$R_{\mathrm{DISS}} = k \times (1-\Omega_c)^n \tag{4}$$

where: k, dissolution rate parameter, 1/time.

Keir (1980) derived a reaction rate order of 4.5 from laboratory dissolution experiments with synthetic calcite. The higher order dependence was challenged by Hales and Emerson (1997a). The authors re-evaluated Keir's (1980) experimental data and concluded that the rate of dissolution is linearly dependent on undersaturation (n=1). According to Hales and Emerson (1997a), the high reaction order derived by Keir (1980) could be attributed to uncertainties in the saturation state of the experimental seawater. Moreover, first-order calcite dissolution kinetics proved to be more consistent with the interpretation of in-situ pore water pH measurements (Hales and Emerson, 1997a, b). As stressed by Gehlen et al. (1999), a satisfying reproduction of pore water profiles through diffusion–reaction models is, however, not a proof per se of the validity of a kinetic expression. Gehlen et al. (2005b) carried out kinetic experiments with biogenic $CaCO_3$. They derived an average reaction rate order of n=2.3±0.4 from 8 experiments with biogenic $CaCO_3$ in artificial seawater. The higher reaction order is explained in terms of a multiphase system. It results from the concomitant dissolution of carbonate fractions characterized by variable reaction rate constants.

While the in-depth discussion of $CaCO_3$ dissolution kinetics is out of the scope of our paper, the preceding section highlights the need for further experimental studies of the dissolution behavior of biogenic $CaCO_3$ phases. For the focus of this modeling study, we adopted a linear dependency of $CaCO_3$ dissolution on undersaturation (n=1). Since the extrapolation of experimental results from controlled laboratory experiments which express reaction rate constants normalized to the specific surface area of $CaCO_3$ (e.g. Keir, 1980; Gehlen et al., 2005b) to the global scale is not straightforward, we used the evolution with depth of $CaCO_3$ fluxes recorded in sediment traps to derive the apparent reaction rate constant k^* (1/time). We selected stations for which mean annual fluxes were reported from at least two different deployment depths from a comprehensive data set on particle fluxes (Dittert et al., 2005). This was the case at 11 stations. In order to derive dissolution rates from $CaCO_3$ fluxes, the time it takes for settling particles to bridge the depth interval between trap deployments needs to be known. This calls for the knowledge of particle sinking speed. The particle sinking speed at depth of trap deployment was obtained from the model parameterization of sinking speed of large particles:

$$w = w_{\min} + (w_{\max} - w_{\min}) \times \max\left(0, \frac{z - z_m}{2000}\right). \tag{5}$$

where: $w_{\min}$, minimum sinking speed of 50 m/d;

$w_{\max}$, sinking speed at 2000 m below the mixed layer of 200 m/d; z, depth; z_m, depth of mixed layer.

Knowing the sinking speed, allows deriving the concentration of $CaCO_3$ from flux observations. The fraction of $CaCO_3$ lost to dissolution was calculated as the difference in $CaCO_3$ concentrations between the respective upper and lower traps. The saturation state of seawater with respect to calcite (Ω_c) was determined from GLODAP data (Key et al., 2004) at the location of the lower trap. At two of the stations even the lower traps were in waters oversaturated with respect to calcite. The slight decrease in $CaCO_3$ fluxes observed in the data suggests either the presence of a more soluble carbonate phase (e.g. aragonite) or shallow dissolution of calcite driven by the interaction between particles and biota (e.g. grazing and dissolution during gut passage or dissolution in acidic microenvironments, see Milliman et al. (1999) for references). Rearranging the model equation for calcite dissolution:

$$R_C = [\mathrm{CaCO_3}] \times k^* \times (1-\Omega_c) \tag{6}$$

$$\text{yields } k^* = \frac{R_c}{[\mathrm{CaCO_3}] \times (1-\Omega_c)}. \tag{7}$$

Terms $[CaCO_3]$ and R_c correspond to the concentration of calcite particles in mol/l, respectively to the bulk dissolution rate in mol/l per unit time. The latter is calculated from the difference in concentrations and the time necessary for settling particles to bridge the depth interval between successive trap deployments.

In a first step k^* was determined for each sediment trap array. This resulted in k^* estimates ranging from 0 to 479.2 d^{-1} with an average value of 93.6 d^{-1} and a median of 12.1 d^{-1}. This wide spread and also the large difference between average and median values suggested a further refinement of the determination of k^*. This fit was done by systematically varying k^* to predict for each sediment trap array the upper $CaCO_3$ concentration from the concentration at the respective lower trap. By systematically varying k^*, the rms-error for the predicted and measured $CaCO_3$ concentrations in the upper traps converged to a minimum value for k^*=10.9 d^{-1}, which was then implemented into the PISCES model.

Possible drawbacks of this approach are that only data from a few stations (11) were available and for two of them calcite dissolution was theoretically impossible due to calcite oversaturation at the lower trap level. This might bias the k^* value towards low estimates, however, these traps contained among the lowest $CaCO_3$ concentrations and thus contributed relatively little error to the optimization of k^* by the rms. Furthermore, the gradient of $CaCO_3$ saturation between the two trap depths was not taken into account, only the degree of saturation at the lower trap level, as at all stations except for one the water surrounding the upper traps was still oversaturated with respect to calcite. This assumption may also bias k^* estimates towards lower values. Fitting k^* by minimization of the rms-error for predictions of the upper trap fluxes may lead to a high weight for traps with high $CaCO_3$ fluxes, as here the misfit between predicted and measured values may have a strong impact on the rms. However, this was obviously not the case as for example the two traps with highest $CaCO_3$ concentrations also had the highest individual k^*-value, but the resulting value for k^* is still relatively low and close to the median.

The flux of $CaCO_3$ reaching the last model box (= lower boundary) is re-dissolved instantaneously after removing the alkalinity equivalent corresponding to river input. The model is strictly mass conserving.

3 Methodology

The 3-D global ocean general circulation model OPA (Madec et al., 1998) provided the physical forcing fields for tracer transport. After 3000 years of integration in an off-line mode at constant pCO_2 of 278 ppm, modeled nutrient and chlorophyll fields have reached a quasi steady-state with yearly mean distributions and seasonal variations similar to observations (Aumont and Bopp, 2006). The new parameterizations of carbonate production and dissolution were implemented into the PISCES standard version and the model was run for another 400 years. This allowed for a reorganization of dissolved inorganic carbon (DIC) and alkalinity (ALK) fields down to 1000 m in response to the modified descriptions of calcification and dissolution. In order to evaluate the potential impact of atmospheric pCO_2 increase on pelagic calcification and $CaCO_3$ dissolution, 3 model experiments were then performed according to the standard CMIP scenario (Coupled Model Intercomparison Progrect, http://www-pcmdi.llnl.gov/projects/cmip/index.php) of atmospheric pCO_2 increasing at a rate of 1% per year from 286 to 1144 ppm over a 140 year time-period. Assuming that under constant climate the land biosphere and the ocean make up for CO_2 sinks of the same order of magnitude (Friedlingstein et al., 2001), the atmospheric pCO_2 increase scenario corresponds to 3320 GtC emitted over the duration of the experiment. In the first simulation, both calcification and dissolution depended on the saturation state of seawater with respect to calcite (CAL01). In the second experiment, calcification was independent of saturation state (= constant at values corresponding to the initial state) and dissolution was allowed to respond to changes in saturation driven by rising pCO_2 (CAL02). A third simulation was set up to isolate the effect of the solubility pump by keeping $CaCO_3$ production and dissolution at preindustrial values (CAL03). All three scenarios were doubled with a corresponding control-run (labeled CTL01 to CTL03) at constant pCO_2. Table 1 summarizes the model simulations carried out.

Table 1. Summary of simulations characteristics.

RUN ID	pCO_2 increase	$CaCO_3$ production dependent on Ω_c	$CaCO_3$ dissolution dependent on Ω_c
CAL01	yes	yes	yes
CTL01	no	yes	yes
CAL02	yes	cst at preind. level	yes
CTL02	no	cst at preind. level	yes
CAL03	yes	cst at preind. level	cst at preind. level
CTL03	no	cst at preind. level	cst at preind. level

4 Results and discussion

4.1 The carbonate cycle in PISCES: Initial state

We plotted the distributions of alkalinity (ALK) and total dissolved inorganic carbon (DIC) along sections across the Atlantic (a), Pacific (c) and Indian Ocean (d) reached at the end of the spin up (pCO_2=278 ppm) on Figs. 2 and 3. Since the model was initialized with the global mean alkalinity concentration by Goyet et al. (2000), we include observed ALK on Figs. 2b, d, f along the same sections. Modeled distributions

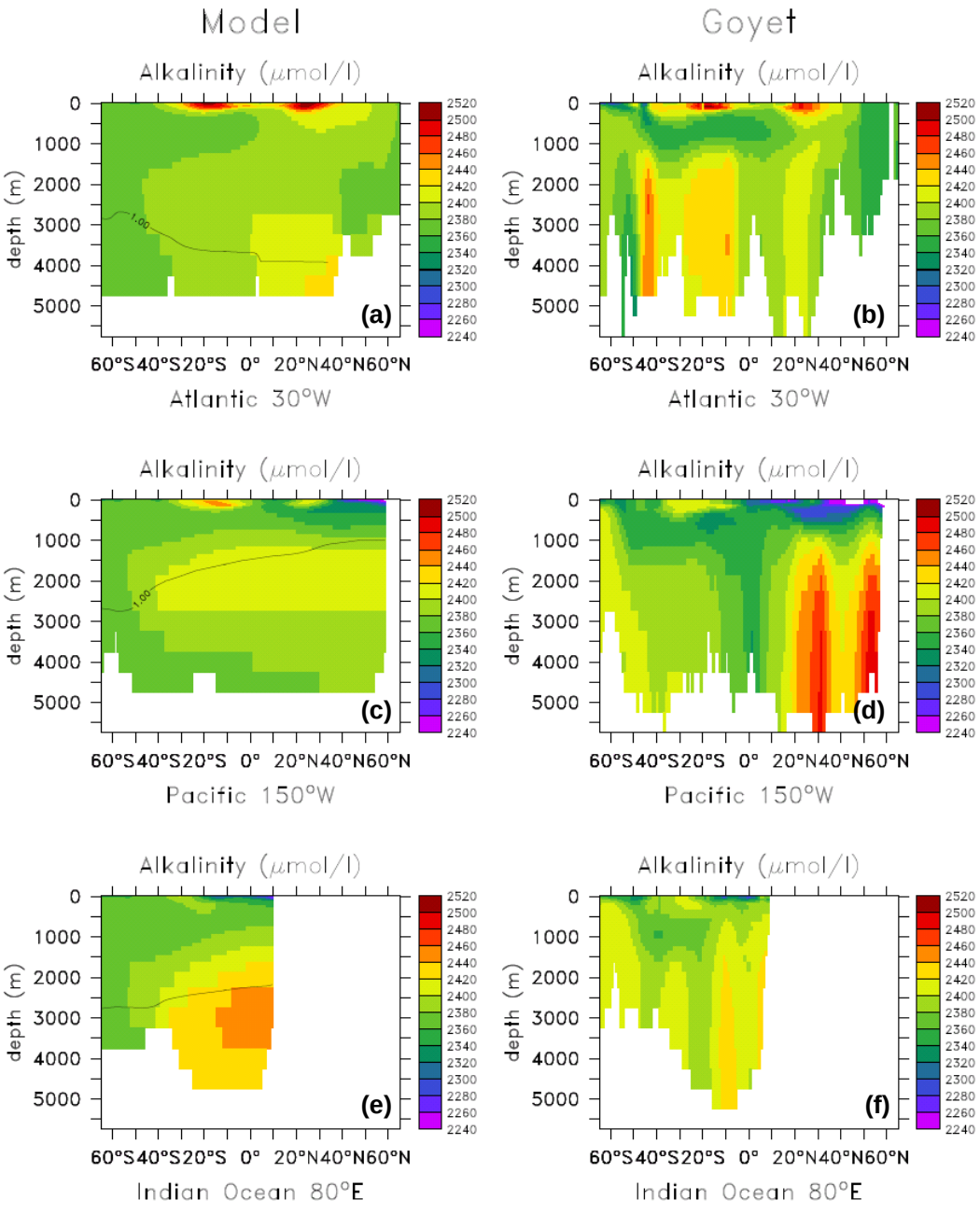

Fig. 2. Comparison between modelled and observed alkalinity (μmol/l) along sections across the Atlantic, Pacific and Indian Ocean: **(a, c, d)**, model output and **(b, d, e)** observations after Goyet et al. (2000). Black line on (a, c, d), predicted depth of the calcite saturation horizon.

of DIC are to the contrary independent of model initialization and reflect internal processes and air-sea gas exchange. We selected preindustrial DIC fields based on the Global Data Analysis Project (GLODAP, Key et al. 2004) for model output – data comparison (Fig. 3b, d, f). The modeled distributions of both tracers reflect the large-scale circulation pattern combined to air-sea gas exchange (DIC) and biological production, as well as remineralization. While the model reproduces the large scale structures of observed DIC fields in all three basins (Fig. 3), a satisfying correspondence between modeled and observed ALK fields is limited to the upper 1000 m of the water column (Fig. 2). Below 1000 m, observed ALK fields display strong latitudinal gradients. These features are not present in the GLODAP data set (Key et al., 2004), neither are they reproduced by the model, which predicts distributional patterns in line with GLODAP. Furthermore, they can not be explained in terms of circulation and/or biological processes. It is likely that they reflect the

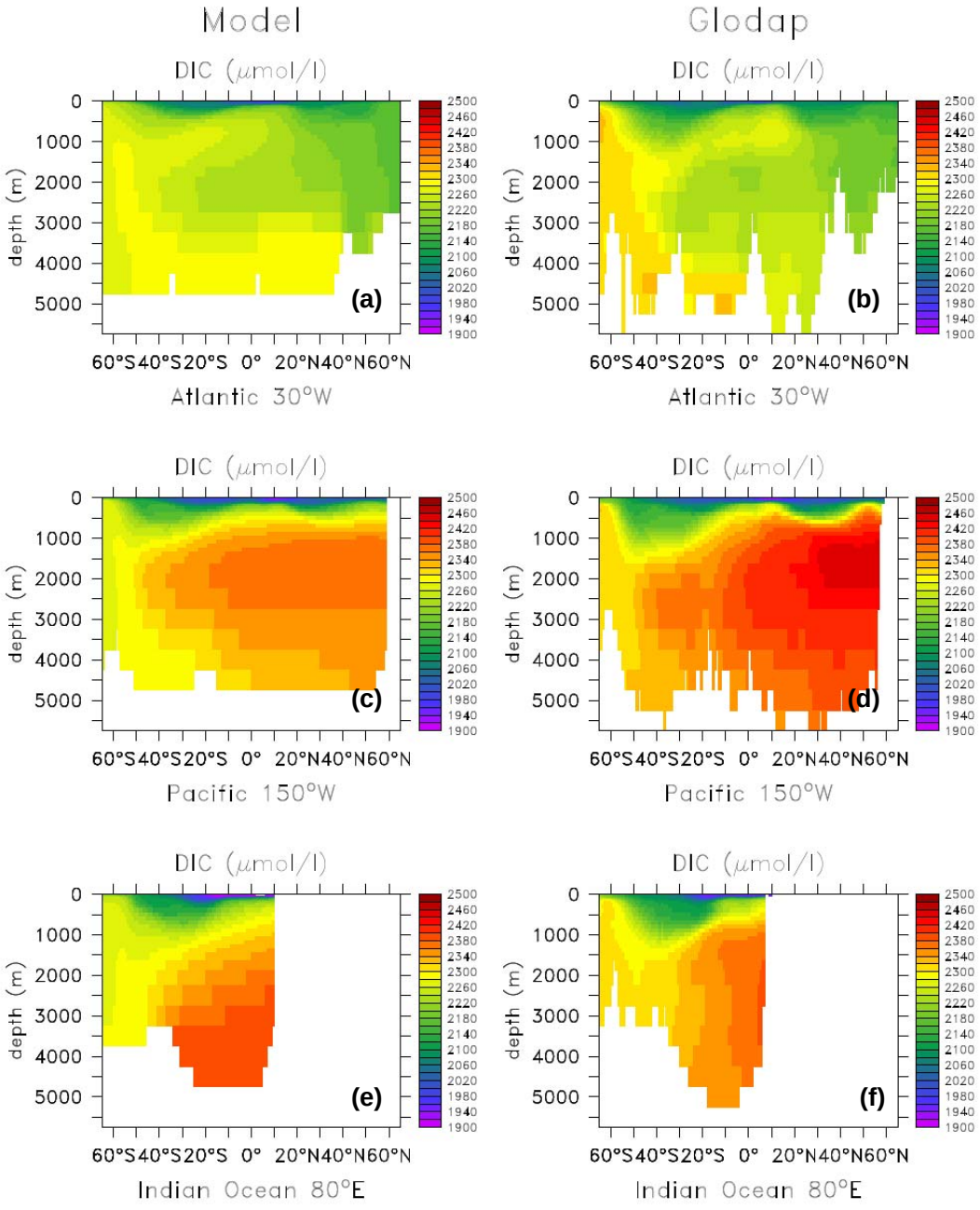

Fig. 3. Comparison between modelled and observed DIC (μmol/l) along sections across the Atlantic, Pacific and Indian Ocean: **(a, c, d)**, model output and **(b, d, e)** observations correspond to pre-industrial concentrations calculated from GLODAP (Key et al., 2004).

underlying method of data interpolation, as the approach used by Goyet et al. (2000) introduces two discontinuities: one at 1000 m and the other at 0° longitude (Key et al., 2004). When limiting our comparison between model output and observation to the upper 1000 m, the model slightly overestimates surface ocean ALK, while it reproduces well the general structure of the fields.

Implementing a dependency for $CaCO_3$ formation on $[CO_3^{2-}]$ and updating the parameterization of $CaCO_3$ dissolution in the model resulted in an improved representation of pre-industrial ALK fields compared to Aumont and Bopp (2006). The former model version predicted even higher surface ocean ALK levels, which together with low $CaCO_3$ export fluxes (Gehlen et al., 2006) suggests an underestimation of the strength of the carbonate counter-pump. The persistent, although smaller overestimation of surface ALK concentrations in the model version used during this study suggests that the amount of dissolution associated with zooplankton grazing (50%) may be too high.

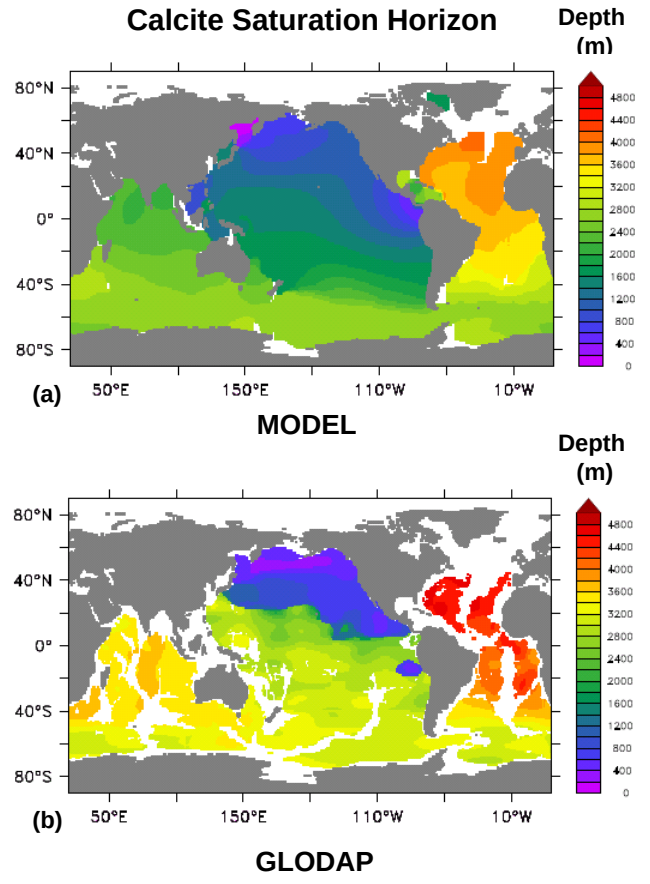

Fig. 4. Depth of calcite saturation horizon: **(a)** model output, **(b)** recalculated from GLODAP (Key et al., 2004).

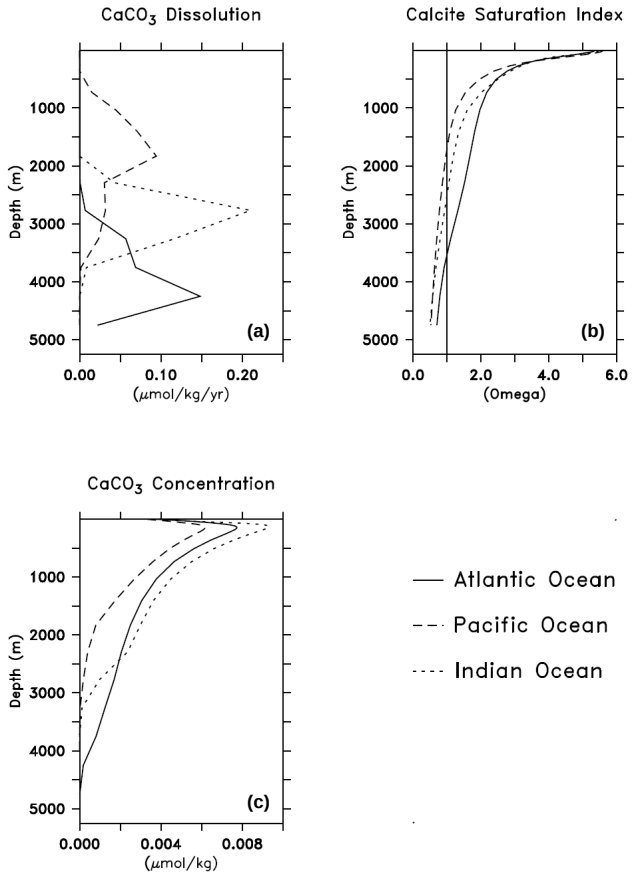

Fig. 5. Basin-wide **(a)** average $CaCO_3$ dissolution rates; **(b)** Saturation index with respect to calcite; **(c)** mean concentration of $CaCO_3$ particles. Note that there are localized areas in the Pacific for which the model predicts a saturation index that is shallower than the basin-wide average of (b).

Figure 4 presents the depth of the calcite saturation horizon predicted by (a) the model and computed for ALK and preindustrial DIC provided by (b) the GLODAP data base (Key et al., 2004). The preindustrial ocean is characterized by a deep calcite saturation horizon in the Atlantic Ocean. In the North Atlantic the entire water column is oversaturated with respect to calcite. The saturation horizon shoals along the flow path of the meridional overturning circulation from North to South across the Atlantic and from South to North in the Pacific, which is captured by the model. We note however that the predicted depth of the saturation horizon is too shallow, which in part reflects the coarse vertical model resolution.

Global rates were computed for the gross, as well as the net carbonate production and carbonate dissolution. They are summarized and compared to literature results in Table 2. The gross $CaCO_3$ production of 1.3 PgC/yr includes the carbonate fraction lost to dissolution during zooplankton grazing. In terms of CO_2 fluxes, the net production (0.8 PgC/yr) is the relevant quantity. It falls at the lower end of published estimates. The model predicts a global dissolution flux of 0.5 PgC/yr and compares well to the estimate given in Feely et al. (2004). The $CaCO_3$ flux at the lower model boundary reflects the boundary conditions and its inherent criteria of mass conservation.

The evolution with depth of the $CaCO_3$ dissolution rate is plotted on Fig. 5a for the Atlantic, Pacific and Indian Ocean. The differences in the evolution with depth of dissolution rates reflect the varying depth of saturation horizon for calcite (Fig. 5b) between ocean basins. Model derived dissolution rates are low compared to in situ dissolution rates summarized by Feely et al. (2004). The distribution of in situ dissolution rates with depth (Fig. 4, Feely et al., 2004) suggests that substantial dissolution occurs for depths <2000 m, which the model fails to reproduce. This does not imply that the global modeled dissolution flux is too low, but rather indicates a discrepancy in the vertical distribution of dissolution predicted by the model and derived from the observations. The missing dissolution at shallow depth is compensated by dissolution below the saturation horizon.

The in situ dissolution rates were estimated from alkalinity fields (excess alkalinity TA*, Feely et al., 2002) and

Table 2. The carbonate cycle in PISCES: Comparison between model ouput and data. All fluxes (production, dissolution) are in Pg $CaCO_3$-C/yr.

Process	Model	Data	Data reference
Mean global DIC (μM)	2292	2305	Key et al. (2004)
Mean global ALK (μM)	2389	2390	Goyet et al. (2002)
Gross $CaCO_3$ production	1.3	0.8–1.4	Igelias-Rodriguez et al. (2002); Lee (2001); Jin et al. (2006); Ridgewell et al. (2007)
Net $CaCO_3$ production	0.8		
Pelagic $CaCO_3$ dissolution	0.5	0.5	Feely et al. (2004)
$CaCO_3$ flux at lower boundary	0.3(1)		
$CaCO_3$ burial flux		0.3	Feely et al. (2004)

(1) From model lower boundary condition.

combine dissolution of calcite and the more soluble carbonate mineral aragonite. Dissolution driven by the upward migration of the calcite and aragonite saturation horizons in response to anthropogenic CO_2 invasion adds to the flux at shallow depth. The model, to the contrary, only simulates calcite and predicts zero dissolution above the calcite saturation horizon. The quantitative contribution of aragonite to the marine $CaCO_3$ cycle awaits further elucidation (Kleypas et al., 2006). Milliman and coworkers (1999) for instance conclude that the shallow water dissolution flux is dominated by the dissolution of calcite. They base their assumption on Fabry's (1990) estimate of the contribution of aragonite to the planktonic $CaCO_3$ production which amounts to only 10%. We demonstrate in a follow-up study that including shallow dissolving aragonite as a model tracer contributes to an improved representation of carbonate geochemistry in the model (Gangstø et al., 2007[1]). However, alkalinity based estimates (Feely et al., 2002) do not account for transport processes in computing excess alkalinity, the latter being totally ascribed to dissolution. Mixing might however transport TA* from below the saturation horizon to shallow depth (Friis et al., 2006). While the occurrence of shallow carbonate dissolution is documented by independent evidence (e.g. Schiebel, 2002), its amount is likely to be overestimated by the TA* technique.

The depth attenuation of $CaCO_3$ fluxes provides an alternative approach to estimate dissolution rates. Feely et al. (2004) compiled data from several trap arrays and computed corresponding dissolution rates. They are smaller than in situ estimates reported in the same paper. Modeled dissolution rates fall within the range of trap derived ones (Feely et al., 2004). The use of sediment trap data has its own sets of caveats (e.g. over-/undertrapping due to turbulence especially for traps deployed at depths $<$1000 m; intrusion of swimmers, hypothesis of a 1-D system etc). Below 1000 m the trapping efficiency of sediment traps is reported to be close to 1 (Yu et al., 2001). We selected only traps deployed at depths $>$1000 m for our analysis. The apparent dissolution rate parameter k^* was derived from $CaCO_3$ flux attenuation profiles and is not a free model parameter. The bulk dissolution rate is the product of the kinetic expression times the concentration of $CaCO_3$ particles (Eq. 6). The average $CaCO_3$ concentration is plotted with depth in Fig. 5c. Feely et al. (2004) used the depth attenuation of $CaCO_3$ fluxes from a different set of trap deployments to derive bulk dissolution rates. The correspondence between modeled dissolution rates and these estimates suggests that the concentration of $CaCO_3$ particles predicted by the model is in the right order of magnitude. To summarize the preceding discussion, the version of the PISCES model just presented computes a carbonate budget within the range of published estimates.

4.2 Transient experiments

Table 3 summarizes simulation results for $CaCO_3$ production, export and dissolution. The reference state of the model presented in the previous section will be referred to as CAL01-1$\times$pCO_2 in the following discussion. Time series of (a) atmospheric pCO_2, (b) mean global $CaCO_3$ (calcite) saturation state of surface ocean waters, (c) net $CaCO_3$ production, (d) $CaCO_3$ export and (e) dissolution, as well as of the (f) cumulative air-sea exchange of CO_2 are reproduced on Fig. 6. Figure 7 presents maps of the saturation state of surface ocean waters with respect to calcite for (a) preindustrial conditions and (b) 4$\times$pCO_2. Model results are presented for net $CaCO_3$ production and $CaCO_3$ dissolution rates integrated over the entire water column in Fig. 8.

The mean global saturation state of surface ocean waters (Fig. 6b) with respect to calcite decrease from $\Omega_c > 5$ at year 0 to Ω_c=2 end the end of the acidification scenario. Maps of Ω_c averaged over the top 100 m of the water column document that the preindustrial ocean is characterized by $\Omega_c > 4$ prevailing between 45° S and 50° N (Fig. 7a), which corresponds according to our parameterization to optimal conditions for calcification. At 4$\times$pCO_2, $\Omega_c < 4$ is predicted everywhere

Table 3. Summary of results. Model output is presented in absolute numbers for experiment CAL01 at $1\times pCO_2$, $2\times pCO_2$ and $4\times pCO_2$. For all experiments, model output is given as drift corrected % change at $4\times pCO_2$ relative to the control simulation at constant pCO_2.

Process	CAL01-$1\times pCO_2$	CAL01-$2\times pCO_2$	CAL01-$4\times pCO_2$	% change CAL01	% change CAL02	% change CAL03
Net $CaCO_3$ production (Pg C/yr)	0.79	0.74	0.58	−27	0	0
$CaCO_3$ export 100 m (Pg C/yr)	0.59	0.55	0.42	−29	−3.6	0
Pelagic dissolution (Pg C/yr)	0.48	0.46	0.42	−16	+19	0

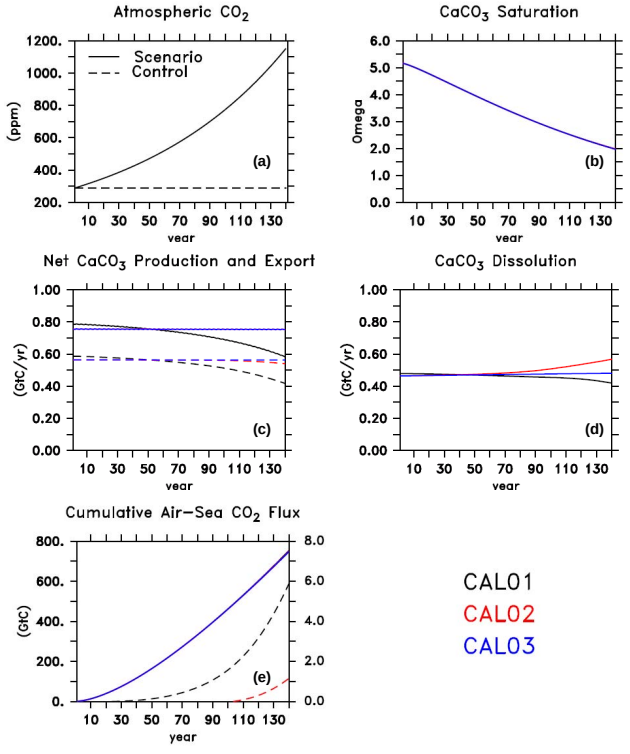

Fig. 6. Time series: **(a)** atmospheric CO_2 (ppm) forcing used for acidification scenarios and control runs; **(b)** mean saturation state of surface ocean waters (0–100 m) with respect to calcite; **(c)** global net $CaCO_3$ production (plain line) and export at 100 m (stippled line); **(d)** global $CaCO_3$ dissolution flux; **(e)** cumulative air-sea flux of CO_2 on left axis, and C uptake in excess to CAL03 on right axis. CAL01 = production and dissolution of $CaCO_3$ responds to changes in carbonate chemistry; CAL02 = constant production, but dissolution responds to changes in carbonate chemistry; CAL03 = constant production and dissolution.

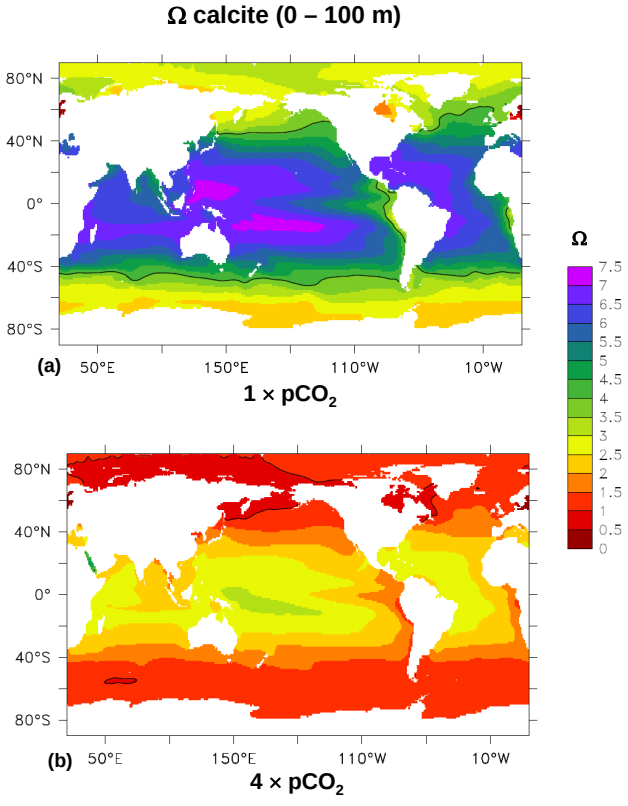

Fig. 7. Saturation state Ω_c with respect to calcite of surface ocean waters (0–100 m): **(a)** $1\times pCO_2$ and **(b)** $4\times pCO_2$. Solid lines indicate Ω_c=4 for $1\times pCO_2$, respectively Ω_c=1 for $4\times pCO_2$.

(Fig. 7b), suggesting suboptimal conditions for pelagic calcification across the global surface ocean.

Net $CaCO_3$ production decreases in response to anthropogenic CO_2 invasion (Fig. 6c) for time series and Fig. 8a, b, c for the spatial distribution). The model predicts a decrease of total production at $2\times pCO_2$ from 0.79 to 0.74 PgC/yr, which further drops to 0.58 PgC/yr at $4\times pCO_2$, yielding a total decrease of 27%. At the same time, the $CaCO_3$ export flux at 100 m (Fig. 6c) decreases by 29% over the course of experiment CAL01. The slightly higher decrease of export flux compared to calcification (27%) reflects the relative increase of dissolution.

The response of $CaCO_3$dissolution to acidification of ocean waters is shown in Fig. 8d to f. Spatial patterns of Fig. 8e and f reflect bottom topography with increasing dissolution along topographic heights (for instance the mid-Atlantic ridge) and decreasing dissolution in the other areas. Since overall less carbonate particles are produced under rising atmospheric pCO_2, their complete dissolution will result

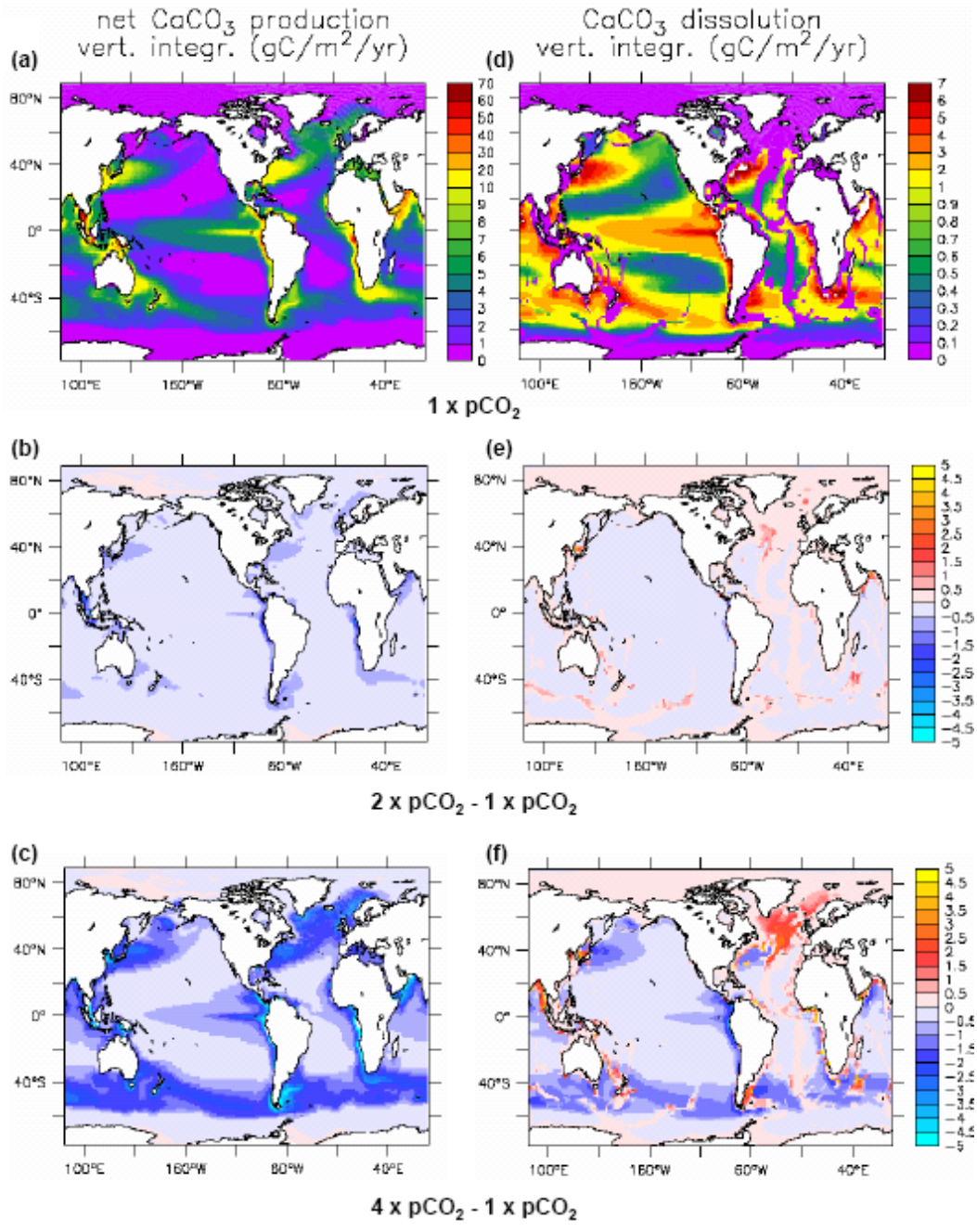

Fig. 8. Net $CaCO_3$ production and $CaCO_3$ dissolution in the simulation CAL01. **(a)** Vertical integrated net production ($gC/m^2/yr$) at $1\times pCO_2$; **(b)** difference in net production at $2\times pCO_2$ minus $1\times pCO_2$; **(c)** difference in net production at $4\times pCO_2$ minus $1\times pCO_2$; **(d)** vertical integrated dissolution rate ($gC/m^2/yr$) at $1\times pCO_2$; **(e)** difference in dissolution rate at $2\times pCO_2$ minus $1\times pCO_2$; **(f)** difference in dissolution rate at $4\times pCO_2$ minus $1\times pCO_2$.

in a lower absolute dissolution flux compared to the preindustrial state. This happens outside areas of benthic $CaCO_3$ accumulation, where at $1\times pCO_2$ close to 100% of the carbonate flux gets dissolved before reaching the benthic boundary layer. In these areas, a shoaling of the saturation horizon will have little to zero impact on total dissolution. To the contrary, in regions with carbonate accumulation, a shoaling of the saturation horizon will result in an increase of the dissolution flux. Relative to total net production, dissolution increases from 61% at $1\times pCO_2$ to 72% at $4\times pCO_2$.

The decrease in calcification in CAL01 goes along with a relative decrease in surface water pCO_2, thereby increasing

the capacity of the ocean for CO_2 uptake. An increase in pelagic $CaCO_3$ dissolution is expected to further enhance this effect due to alkalinity production. However, the lower flux of carbonate particles translates in an overall lower absolute dissolution flux (−16%, Table 3 and Fig. 6e), which partially counteracts the effect of decreasing production on air-sea CO_2 exchange. The combination of processes results in a net increase of the oceanic DIC inventory from 35 578 to 36 421 Gt C (=2.1%). In the experiment CAL02, where carbonate production was constant at preindustrial levels, we compute a net increase in dissolution of 19% (Table 3 and Fig. 6e). The effect of dissolution alone results in a DIC inventory increase of the same order of magnitude as for CAL01. This result stresses the importance of changes in $CaCO_3$ dissolution in addition to production, in controlling the magnitude of the full $CaCO_3$ feedback on atmospheric CO_2 increase.

Changes in DIC inventories computed for experiments CAL01 and CAL02 reflect the combined response of the solubility pump and $CaCO_3$ production and dissolution to increasing atmospheric pCO_2. Experiment CAL03 during which carbonate production and dissolution were kept constant at pre-industrial levels allows the contribution of the solubility pump to be singled out. During experiment CAL01, the cumulative uptake of CO_2 by the ocean in excess to the solubility pump is 5.9 GtC (Fig. 6e). In contrast with CAL01, constant calcification and increasing dissolution in CAL02 combine into an additional 1.2 GtC taken up in excess to CAL03 (Fig. 6e). Consequently, the effect of reduced calcification in CAL01 enhances the negative feedback to rising atmospheric CO_2 compared to CAL02, where only dissolution is at work. The cumulative ocean uptake of CO_2 of 5.9 GtC during experiment CAL01 is low compared to the total change in DIC inventory of about 750 GtC. It should however not preclude the expected consequence for the entire pelagic ecosystem.

4.3 Comparison of assessments of future changes in marine calcification

Heinze (2004) predicts a global decrease in $CaCO_3$ of 50% at the end of a model experiment similar to CAL01. The final atmospheric CO_2 concentration was however higher than $4\times pCO_2$. At $4\times pCO_2$, carbonate production declined by approximately 38 % (Fig. 3 in Heinze, 2004) compared to 27% in this study. While Heinze (2004) used different forcing scenarios, the discrepancy in the predicted sensitivity of calcification to acidification is most likely due to differences in the parameterizations of $CaCO_3$ production and its dependency on pCO_2. Heinze (2004) lets the $CaCO_3$ production be linearly dependent on seawater pCO_2. It is however likely that the biological response is not linear with pCO_2, but rather follows an asymptotic type function. It is thus likely that Heinze (2004)'s estimate corresponds to an upper limit of the decrease of carbonate production in response to increasing pCO_2.

Ridgwell et al. (2007a) reach the opposite conclusion, namely that Heinze's (2004) estimate would be the lower limit of the expected response. They point to the potential bias introduced by parameterizations based on experimental results obtained for *Emiliania huxleyi*. Ridgwell et al. (2007a) compiled experimental data documenting the calcification response of different organisms to increasing pCO_2. They fitted data from individual experiments (e.g. Bijma et al., 1999) or group of experiments (e.g. Zondervan et al., 2001) to the widely accepted rate expression of $CaCO_3$ precipitation

$$R_{\mathrm{PREC}} = k \times (1 - \Omega_c)^n. \quad (8)$$

Inorganic precipitation of calcium carbonate is known to follow Eq. (8) (Zhong and Mucci, 1993, and references therein). The reaction rate order n determined for inorganic precipitation is strictly $\geq$1. Interestingly, with the exception of corals for which a value of $n\sim$1 was determined, Ridgwell et al. (2007a) derived values of n ranging from 0.2 to 0.75 from biogenic calcification experiments. Previous studies (Hales and Emerson, 1997; Gehlen et al., 2005) highlighted potential sources of uncertainty in the determination of the reaction rate order from the reassessment of experimental data. Whether values of $n<1$ are a true characteristic of biotic calcification or an artifact introduced by fitting Eq. (8) to a limited set of scattered data needs further experimental elucidation.

The potential for a variable reaction of different calcifying species to ocean acidification needs to be stressed. Langer et al. (2006) report data on the calcification response of the coccolithphores *Calcidiscus leptoporus* and *Coccolithus pelagicus* to increased pCO_2. While to former displays an optimum curve centered at present day pCO_2 ($\sim$360 ppm), the later appears rather invariant to pCO_2 increase. The relationship between calcification and pCO_2 in *C. leptoporus* suggests decreased rates of PIC production during past periods of lower atmospheric pCO_2. Since decreased rates of PIC production correlate with changes in coccolith morphology (Langer et al., 2006), the analysis of the sedimentary record provides a means for the verification of this hypothesis. Langer et al. (2006) analyzed *C. leptoporus* liths from last glacial maximum and Holocene sediments and found no evidence for changes in coccolith morphology. The inconsistency between results obtained from laboratory experiments and analysis of geological samples, might indicate the adaptation of *C. leptoporus* to changes in carbonate chemistry. The impact of ocean acidification on marine calcifiers will ultimately depend on their capability to adapt. In this context, understanding the differential response of coccolithophore species to pCO_2 challenges our knowledge of the controls of biomineralization processes. The scenario CAL02 can be considered as an extreme end-member for the unlikely situation of 100% success in adaptation of pelagic calcifiers to

changes in carbonate chemistry. Under these circumstances only inorganic dissolution would respond to decreasing saturation state.

Next to adaptation at the species level, changes in community composition driven by the differential response of species to changing carbonate chemistry are likely to occur (Riebesell et al., 2000; Zondervan et al., 2001; Langer et al., 2006). Henderiks and Rickaby (2006) propose an evolutionary explanation to the emerging pattern of differences between species in pCO_2 tolerance. Following this line of thought, the differential tolerance of coccolithophore species reflects the conditions under which the species emerged in the past. If this hypothesis is confirmed, changes in carbonate chemistry might result in changes in species composition of calcifying communities, rather than in their decline. In such a scenario, the cosmopolitan *E. huxleyi* might be outcompeted by *C. pelagicus*. The replacement of a species by another, even within a single functional type (e.g. pelagic calcifying autotroph), is likely to affect the ecosystem as a whole. Processes like adaptation and competition between species challenge our predictive capability of the biogeochemical, respectively ecological impacts of ocean acidification.

5 Conclusions

The biogeochemical model PISCES was updated to include a dependency of $CaCO_3$ production on the saturation of seawater with respect to calcite and a revised parameterization of $CaCO_3$ dissolution. The model reproduces a marine carbonate cycle largely consistent with independent estimates. The model underestimates $CaCO_3$ dissolution between 0 and 2000 m, which can in part be attributed to the fact that the model only considers calcite.

Model experiments were carried out in order to quantify the evolution of $CaCO_3$ production and dissolution under conditions of increasing atmospheric CO_2. Carbonate production decreased by 27% in response to a pCO_2 increase of 1% per year from the preindustrial value of 286 ppm to $4\times pCO_2$. Our study highlights the contribution of $CaCO_3$ dissolution to the feedback on increasing atmospheric pCO_2. Taken individually, the relative increase of dissolution in response to acidification drives an excess uptake of CO_2 from the atmosphere of 1.2 GtC over the time span of the experiment. The combined changes in $CaCO_3$ production and dissolution lead to 5.9 GtC transferred from the atmosphere to the ocean in excess to the solubility pump. Although this effect is low compared to the total change in DIC inventory of about 750 GtC, it should not hide the potential for major changes in ecosystem structure. The decrease in surface ocean saturation with respect to calcite threatens the competitiveness of pelagic calcifiers, among which *E. huxleyi* might be particularly vulnerable (Hendericks and Rickaby, 2006). A shift in species composition is likely to affect the entire food chain up to commercial fish. Associated changes in export production will modify the downward delivery of POC and thereby the availability of energy for the deep ocean and benthos.

Acknowledgements. This work was supported through EU grants 511106-2 (FP6 RTD project EUR-OCEANS) and GOCE-511176 (FP6 RTP project CARBOOCEAN) by the European Commission. M. G. acknowledges a visiting fellowship be the Hanse Institut for Advanced Study (Delmenhorst/Germany). This is publication number 2503 from LSCE.

Edited by: J. Middelburg

References

Arakaki, T. and Mucci, A.: A continuous and mechanistic representation of calcite reaction-controlled kinetics in dilute solutions at 25°C and 1 atm total pressure, Aqu. Geochem., 1, 105–130, 1995.

Archer, D. and Maier-Reimer, E.: Effect of deep-sea sedimentary calcite preservation on atmospheric CO_2 concentration, Nature, 367, 260–263, 1994.

Armstrong, R. A., Lee, C., Hedges, J. I., Honjo, S., and Wakeham, S. G.: A new, mechanistic model for organic carbon fluxes in the ocean: based on the quantitative association of POC with ballast minerals, Deep-Sea Res. II, 49, 219–236, 2002.

Aumont, O. and Bopp, L.: Globalizing results from ocean in situ iron fertilization studies, Global Biogeochem. Cy., 20, GB2017, doi:10.1029/2005GB002591, 2006.

Aumont, O., Maier-Reimer, E., Blain, S., and P. Monfray, P.: An ecosystem model of the global ocean including Fe, Si, P colimitations, Global Biogeochem. Cy., 17(2), 1060, doi:10.1029/2001GB001745, 2003.

Berner, R. A.: The solubility of calcite and aragonite in seawater at atmospheric pressure and 34.5% salinity, Am. J. Sci., 276, 713–730, 1976.

Berner, R. A. and Morse, J. W.: Dissolution kinetics of calcium carbonate in seawater. IV. Theory of calcite dissolution, Am. J. Sci. 274, 108–134, 1974.

Bijma, J., Spero, H. J., and Lea, D. W.: Reassessing foraminiferal stable isotope geochemistry: Impact of the oceanic carbonate system (Experimental Results), in: Use of proxies in paleoceanography: Examples from the South Atlantic, edited by: Fischer, G. and Wefer, G., 20 Springer-Verlag Berlin Heidelberg, 489–512, 1999.

Bopp, L., Kohfield, K. E., Quéré, C. L., and O. Aumont, O.: Dust impact on marine biota and atmospheric pCO_2 during glacial periods, Paleoceanogr., 18(2), 1046, doi:10.1029/2002PA000810, 2003.

Caldeira, C. and Wickett, M. E.: Anthropogenic carbon and ocean pH, Nature, 425, 365, doi:10.1038/425365a, 2003.

Chou, L., Garrels, R. M., and Wollast, R.: A comparative study of the kinetics and mechanisms of dissolution of carbonate minerals, Chem. Geol., 78, 269–282, 1989.

Delille, B., Harlay, J., Zondervan, I., Jacquet, S., Chou, L., Wollast, R., Bellerby, R. G. J., Frankignoulle, M., Borges, A. V., Riebesell, U., and Gattuso, J.-P.: Response of primary production and calcification to changes of pCO_2 during experimental

blooms of the coccolithophorid Emiliania huxleyi, Global Biogeochem. Cy., 19, GB2023, doi:10.1029/2004GB002318, 2005.

Dittert, N., Corrin, L., Bakker, D., Bendtsen, J., Gehlen, M., Heinze, C., Maier-Reimer, E., Michalopoulos, P., Soetaert, K. E. R., and Tol, R. J. S.: Integrated Data Sets of the FP5 Research Project ORFOIS: Origin and fate of biogenic particle fluxes in the ocean and their interactions with atmospheric CO_2 concentrations as well as the marine sediment, Vol. 1, WDC-MARE Reports 0002, 2005.

Fabry, V. J.: Aragonite production by pteropod mollusks in the subarctic Pacific, Deep-Sea Res., 36(11), 1735–1751, 1989.

Fabry, V. J.: Shell growth rates of pteropods and heteropod mollusks and aragonite production in the open ocean: Implications for the marine carbonate system, J. Mar. Res., 48, 209–222, 1990.

Feely, R. A., Sabine, C. L., Lee, K., Millero, F. J., Lamb, M. F., Greeley, D., Bullister, J. L., Key, R. M., Peng, T.-H., Kozyr, A., Ono, T., and Wong, C. S.: In situ calcium carbonate dissolution in the Pacific Ocean, Global Biogeochem. Cy., 16(4), 1144, doi:10.1029/2002GB001866, 2002.

Feely, A., Sabine, C. L., Lee, K., Berelson, W., Kleypas, J., Fabry, V. J., and Millero, F. J.: Impact of Antropogenic CO_2 on the $CaCO_3$ System in the Oceans, Science, 305, 362–366, 2004.

Frankignoulle, M., Canon, C., and Gattuso, J.-P.: Marine calcification as a source of carbon dioxide: Positive feedback of increasing atmospheric CO_2, Limnol. Oceanogr., 39(2), 458–462, 1994.

Friedlingstein, P., Dufresne, J.-L., Cox, P. M., and Rayner, P.: How positive is the feedback between climate change and the carbon cycle?, Tellus B, 55(2), 692–700, doi:10.1034/j.1600-0560.2003.01461.x 2001.

Friis, K., Najjar, R. G., Follows, M. J., and Dutkiewicz, S.: Possible overestimation of shallow-depth calcium carbonate dissolution in the ocean, Global Biogeochem. Cy., 20, GB4019, doi:10.1029/2006GB002727, 2006.

Gattuso, J.-P., Frankignoulle, M., Bourge, I., Romaine, S., and Buddemeier, R. W.: Effect of calcium carbonate saturation of seawater on coral calcification, Global Planet. Change, 18, 37–46, 1998.

Gehlen, M., Mucci, A., and Boudreau, B.: Modelling the distribution of stable carbon isotopes in porewaters of deepsea sediments, Geochim. Cosmochim. Acta, 63, 2763–2773, 1999.

Gehlen, M., Bassinot, F. C., Chou, L., and McCorkle, D.: Reassessing the dissolution of marine carbonates: I. Solubility, Deep Sea Res. I, 52(8), 1445–1460, doi:10.1016/j.dsr.2005.03.010, 2005a.

Gehlen, M., Bassinot, F. C., Chou, L., and McCorkle, D.: Reassessing the dissolution of marine carbonates. Part II: reaction kinetics, Deep-Sea Res. I, 52(8), 1461–1476, doi:10.1016/j.dsr.2005.03.011, 2005b.

Gehlen, M., Bopp, L., Emprin, N., Aumont, O., Heinze, C., and Ragueneau, O.: Reconciling surface ocean productivity, export fluxes and sediment composition in a global biogeochemical ocean model, Biogeosciences, 3, 521–537, 2006, http://www.biogeosciences.net/3/521/2006/.

Goyet, C., Healy, R., and Ryan, J.: Global distribution of total inorganic carbon and total alkalinity below the deepest winter mixed layer depths, Carbon Dioxide Information Analysis Center, Oak Ridge National Laboratory, U.S. Department of Energy, Tennessee, 2000.

Gruber, N., Friedlingstein, P., Field, C. B., Valentini, R., Heimann, M., Richey, J. E., Romero-Lankao, P., Schulze, D., and Chen, C.-T. A.: The vulnerability of the carbon cycle in the 21st century: An assessment of carbon-climate-human interactions, in: The Global Carbon Cycle: Integrating Humans, Climate, and the Natural World, edited by: Field, C. B. and Raupach, M. R., Island Press, Washington, D.C., 45–76, 2004.

Hales, B. and Emerson, S.: Evidence in support of first-order dissolution kinetics of calcite in seawater, Earth Planet. Sci. Lett., 148, 317–327, 1997a.

Hales, B. and Emerson, S.: Calcite dissolution in sediments of the Ceara Rise: in situ measurements of porewater O_2, pH, and $CO_{2(aq)}$, Geochim. Cosmochim. Acta, 61, 504–514, 1997b.

Henderiks, J. and Rickaby, R. E. M.: A coccolithophore concept for constraining the Cenozoic carbon cycle, Biogeosciences, 4, 323–329, 2007, http://www.biogeosciences.net/4/323/2007/.

Heinze, C.: Simulating oceanic $CaCO_3$ export production in the greenhouse, Geophys. Res. Let., 31, L16308, doi:10.1029/2004GL020613, 2004.

Honjo, S. and Erez, J.: Dissolution rates of calcium carbonates in the deep ocean: an in-situ experiment in the North Atlantic Ocean, Earth Planet. Sci. Lett., 40, 287–300, 1978.

Iglesias-Rodriguez, M. D., Armstrong, R., Feely, R., Hood, R., Kleypas, J., Milliman, J. D., Sabine, C., and Sarmiento, J.: Progress made in study of ocean's calcium carbonate budget, EOS, 83(34), 365, 374–375, 2002.

Ittekott, V.: The abiotically driven biological pump in the ocean and short-term fluctuations in atmospheric CO_2 contents, Global Planet. Change, 8, 17–25, 1993.

Ingle, S. E., Culberson, C. H., Hawley, J. B., and Pytkowicz, R. M.: The solubility of calcite in sea water at atmospheric pressure and $35\%_0$ salinity, Mar. Chem., 1, 295–307, 1973.

Jackson, G. A.: A model for the formation of marine algal flocs by physical coagulation processes, Deep Sea Res., 37, 1197–1211, 1990.

Jin, X., Gruber, N., Dunne, J. P., Sarmiento, J. L., and Armstrong, R. A.: Diagnosing the contribution of phytoplankton functional groups to the production and export of particulate organic carbon, CaCO3, and opal from global nutrient and alkalinity distributions, Global Biogeochem. Cy., 20, GB2015, doi:10.1029/2005GB002532, 2006.

Klaas, C. and Archer, D. E.: Association of sinking organic matter with various types of mineral ballast in the deep sea: Implications for the rain ratio, Global Biogeochem. Cy., 16(4), 1116, doi:10.1029/2001GB001765, 2002.

Keir, R. S.: The dissolution kinetics of biogenic carbonate in seawater, Geochim. Cosmochim. Acta, 44, 241–252, 1980.

Key, R. M., Kozyr, A., Sabine, C. L., Lee, K., Wanninkhof, R., Bullister, J. L., Feely, R. A., Millero, F. J., Mordy, C., and Peng, T.-H.: A global ocean carbon climatology: Results from Global Data Analysis Project (GLODAP), Global Biogeochem. Cy., 18, GB4031, doi:10.1029/2004GB0022, 2004.

Kleypas, J. A., Buddemeier, R. W., Archer, D., Gattuso, J.-P., Langdon, C., and Opdyke, B. N.,: Geochemical consequences of increased atmospheric CO_2 on coral reefs, Science, 284, 118–120, 1999.

Kleypas, J. A., Feely, R. A., Fabry, V. J., Langdon, C., Sabine, C. L., and Robbins, L. L.: Impacts of ocean acidification on coral reefs and other marine calcifiers: A guide for future research,

Report of a workshop sponsored by NSF, NOAA and the U.S. Geological Survey, 88 pp., 2006.

Kriest, I. and Evans, G. T.: Representing phytoplankton aggregates in biogeochemical models, Deep Sea Res. I, 46, 1841–1859, 1999.

Kriest, I. and Evans, G. T.: A vertically resolved model for phytoplankton aggregation, Proc. Indian Acad. Sci. Earth Planet. Sci., 109, 453–469, 2000.

Langer G., Geisen, M., Baumann, K.-H., Kläs, J., Riebesell, U., Thoms, S., and Young, J. R.: Species-specific responses of calcifying algae to changing seawater carbonate chemistry, Geochem. Geophys. Geosyst., 7, Q09006, doi:10.1029/2005GC001227, 2006.

Lee, K.: Global net community production estimated from the annual cycle of surface water total dissolved inorganic carbon, Limnol. Oceanogr., 46(6), 1287–1297, 2001.

Lewis, E. and Wallace, D. W. R.: Program Developed for CO_2 System Calculations. ORNL/CDIAC-105, Carbon Dioxide Information Analysis Center, Oak Ridge National Laboratory, U.S. Department of Energy, Tennessee, 1998.

Madec, G. P., Delecluse, P., Imbard, M., and Lévy, C.: OPA 8.1 Ocean general circulation model reference manual, Notes du pole de modélisation, IPSL, 1998.

Mehrbach, C., Culberson, C. H., Hawley, J. E., and Pytkowicz, R. M.: Measurement of the apparent dissociation constant of carbonic acid in seawater at atmospheric pressure, Limnol. Oceanogr., 18, 897–907, 1973.

Milliman, J. D., Troy, P. J., Balch, W. M., Adams, A. K., Li, Y.-H., and Mackenzie F. T.: Biologically mediated dissolution of calcium carbonate above the chemical lysocline?, Deep-Sea Res. I, 46, 1653–1669, 1999.

Moore, J. K., Doney, S. C., Kleypas, J. A., Glover, D. M., and Fung, I. Y.: An intermediate complexity marine ecosystem model for the global domain, Deep-Sea Res. II, 49, 403–462, 2002.

Morse, J. W.: Dissolution kinetics of calcium carbonate in seawater. VI. The near-equilibrium dissolution kinetics of carbonate-rich deep-sea sediments, Am. J. Sci., 278, 344–353, 1978.

Morse, J. W. and Arvidson, R. S.: The dissolution kinetics of major sedimentary carbonate minerals, Earth-Sci. Rev., 58, 51–84, 2002.

Morse, J. W. and Berner, R. C.: Dissolution kinetics of calcium carbonate in sea water. II: a kinetic origin for the lysocline, Am. J. Sci., 272, 840–851, 1972.

Mucci, A.: The solubility of calcite and aragonite in seawater at various salinities, temperatures and one atmosphere total pressure, Am. J. Sci., 283, 780–799, 1983.

Orr, J. C., Fabry, V. J., Aumont, O., Bopp, L., Doney, S. C., Feely, R. A., Gnanadesikan, A., Gruber, N., Ishida, A., Joos, F., Key, R. M., Lindsay, K., Maier-Reimer, E., Matear, R., Monfray, P., Mouchet, A., Najjar, R. G., Plattner, G.-K., Rodgers, K. B., Sabine, C. L., Sarmiento, J. L., Schlitzer, R., Slater, R. D., Totterdell, I. J., Weirig, M.-F. , Yamanaka, Y., and Yool, A.: Antropogenic ocean acidification over the twenty-first century and its impact on calcifying organisms, Nature, 437, 681–686, 2005.

Plummer, L. N., Wigley, T. M. L., and Parkhurst, D. L.: The kinetics of calcite dissolution in CO_2-water systems at 5–60°C and 0.0 to 1.0 atm CO_2, Am. J. Sci., 278, 179–216, 1978.

Ridgwell, A., Zondervan, I., Hargreaves, J. C., Bijma, J., and Lenton, T. M.: Significant long-term increase of fossil fuel CO_2 uptake from reduced marine calcification, Biogeosciences, 4, 481–492, 2007a.

Ridgwell, A., Hargreaves, J. C., Edwards, N. R., Annan, J. D., Lenton, T. M., Marsh, R., Yool, A., and Watson, A.: Marine geochemical data assimilation in an efficient Earth System Model of global biogeochemical cycling, Biogeosciences, 4, 87–104, 2007b.

Riebesell, U., Zondervan, I., Rost, B., Tortell, P. D., Zeebe, R. E., and Morel, F. M. M.: Reduced calcification of marine plankton in response to increased atmospheric CO_2, Nature, 407, 364–368, 2000.

Sabine, C. L., Feely, R. A., Gruber, N., Key, R. M., Lee, K., Bullister, J. L., Wanninkhof, R., Wong, C. S., Wallace, D. W. R., Tilbrook, B., Millero, F. J., Peng, T.-H., Kozyr, A., Ono, T., and Rios, A. F.: The oceanic sink for anthropogenic CO_2, Science, 3005, 367–370, 2004.

Schiebel, R.: Planktic foraminiferal sedimentation and the marine calcite budget, Global Biogeochem. Cy., 16, 1065, doi:10.1029/2001GB001459, 2002.

Sciandra, A., Harlay, J., Lefèvre, D., Lemée, R., Rimmelin, P., Denis, M., and Gattuso, J.-P.: Response of coccolithophorid *Emiliania huxleyi* to elevated partial pressure of CO_2 under nitrogen limitation, Mar. Ecol. Prog. Ser., 261, 111–122, 2003.

Walter, L. M. and Morse, J. W.: The dissolution kinetics of shallow marine carbonates in seawater: a laboratory study, Geochim. Cosmochim. Acta, 49, 1503–1514, 1985.

Zeebe, R. E. and Wolf-Gladrow, D.: CO_2 in seawater: Equilibrium, kinetics, isotopes, Elsevier Oceanography Series, 65, 346 pp., 2001.

Zhong, S. J. and Mucci, A.: Calcite precipitation in seawater using a constant addition technique – a new overall reaction kinetic expression, Geochim. Cosmochim. Acta, 57, 1409–1417, 1993.

Zondervan, I., Zeebe, R. E., Rost, B., and Riebesell, U.: Decreasing marine biogenic calcification: A negative feedback on rising atmospheric pCO_2, Global Biogeochem. Cy., 15, 2, 507–516, 2001.

Zondervan, I., Rost, B., and Riebesell, U.: Effect of CO_2 concentration on the PIC/POC ratio in the coccolithophore Emiliania huxleyi grown under light-limiting conditions and different daylengths, J. Exp. Mar. Biol. Ecol., 272, 55–70 2002.